Regular Article

PHYSICAL CHEMISTRY RESEARCH
Published by the
Iranian Chemical Society
www.physchemres.org
info@physchemres.org

***Phys. Chem. Res.**, Vol. 3, No. 3, 205-216, September 2015.*
DOI: 10.22036/pcr.2015.9575

Thermodynamics Binding of Tetrakis (2,3,5,6-Tetrafluoro-N,N′,N″-Trimethyl Ammonium Phenyl) Porphyrin Nickel(II) With Calf Thymus DNA

N. Sohrabi*, N. Rasouli and F. Fateminasab
Department of Chemistry, Payame Noor University, P.O. Box 19395-3697, Tehran, Iran
(Received 13 February 2015, Accepted 13 May 2015)

In this study, aggregation behavior of a water soluble cationic metalloporphyrin, meso-tetrakis (2,3,5,6-tetrafluoro-N,N´,N´´-trimethyl ammonium phenyl) porphyrin nickel(II) [Ni(II)(TF_4TMAPP)]$^{4+}$ is investigated in 5 mM aqueous phosphate buffer of pH 7.0 at 25.0 °C and various ionic strengths using optical absorption and resonance light scattering spectroscopic methods. The results suggest that [Ni(II)(TF_4TMAPP)]$^{4+}$ do not aggregate in the experimental concentration range. Also, the interaction of cationic metalloporphyrin, [Ni(II)(TF_4TMAPP)]$^{4+}$ with calf thymus DNA (ct-DNA) is studied in 5 mM aqueous phosphate buffer of pH 7.0 by optical absorption, resonance light scattering (RLS), fluorescence spectroscopy and thermal denaturation measurements. The binding constants are determined by analysis of the optical absorption spectra of the [Ni(II)(TF_4TMAPP)]$^{4+}$ at various temperatures using SQUAD software. The thermodynamic parameters are also calculated by van't Hoff equation. The results indicate that the process is entropy-driven and suggest that the main driving forces are the outside binding mode.

Keywords: Cationic metalloporphyrin, CT-DNA, Thermodynamic parameters, SQUAD

INTRODUCTION

Cationic metalloporphyrins and their non-covalent interaction with DNA have been the subject of intense investigations on molecular recognition since their first synthesis and their prior discovery by Fiel *et al.* [1,2]. Based on recent reports, cationic porphyrins, in biological systems, act as an inhibitor of human telomerase [3], receptor for peptides [4], DNA cleaver [5] and a specific probe of DNA structure [6]. The interaction between DNA and cationic metalloporphyrins has been studied intensively for its unique physicochemical properties in interaction with nucleic acid [7,8]. Generally, three major binding modes have been proposed for the binding of cationic metalloporphyrins to DNA: intercalation, outside groove binding and outside binding with self-stacking, in which porphyrins are stacked along the DNA helix [9,10]. The binding mode could be modulated by the nature of the metal, size and location of the substitution groups on the periphery of the porphyrin. Generally, free bases and square planar complexes such as Ni^{2+} and Cu^{2+} intercalate between DNA base pairs. For the metalloporphyrins having axially bound ligands such as Co^{3+}, Mn^{3+} and Fe^{3+} or those with bulky substituents on the periphery of the structure, intercalation is blocked and outside binding occurs [11,12]. The extensive exploration of cationic porphyrins has been hitherto limited to the porphyrins with pyridinium and anilinium groups as meso-substituents [13-15]. The meso-substituted cationic porphyrins form a class of molecules that have been shown to interact with duplex oligonucleotides, either by external binding with or without self-stacking, presumably as a result of a charge interaction with nucleic acid phosphate and/or by partial or full intercalation depending on the identity of the porphyrin [16-18]. These molecules have been used as probes to investigate the structure of nucleic acids. They are effective tumor-localizing agents [19,20] and have been used in treatment and detection of a number of cancers. The binding

*Corresponding author. E-mail: sohrabnas@pnu.ac.ir

strength of porphyrin to DNA is one of the important parameters on its efficacy. The thermodynamic parameters of binding can also help us to obtain more insight into the molecular nature of interactions. Hence, determination of thermodynamic parameters governing DNA-porphyrin complex formation makes deeper insight into the molecular basis of DNA-porphyrin interactions. On the basis of this importance, in present study, the interaction of a new meso-substituted tetracationic metalloprphyrin, meso-tetrakis (2,3,5,6-tetrafluoro-N, N´,N´´-trimethyl ammonium phenyl) porphyrin Nickel(II), $[Ni(II)(TF_4TMAPP)]^{4+}$ (Scheme 1) with calf thymus deoxy ribose nucleic acid (ct-DNA) has been studied in view of thermodynamics using various techniques such as UV-Vis absorption, fluorescence spectroscopy, resonance light scattering spectroscopy (RLS) and thermal denaturation measurements. Running the interaction experiments at various temperatures, let us to estimate all of the thermodynamic parameters of interactions and obtain useful information regard binding mechanism.

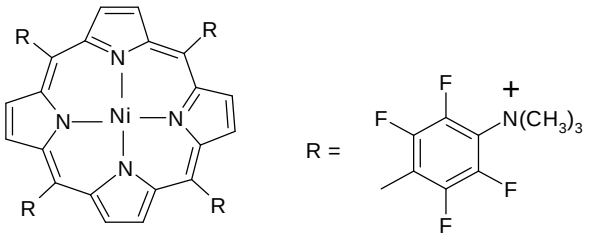

Scheme 1. The structure of meso-tetrakis (2,3,5,6 tetrafluoro-N,N´,N´´-trimethyl ammonium phenyl) porphyrin nickel(II)

EXPERIMENTAL

Chemicals and Preparations

Calf thymus DNA was purchased from Sigma. The water soluble cationic metalloporphyrin, $[Ni(II)(TF_4TMAPP)]^{4+}$ was prepared and purified according to literature methods [21,22]. This metalloporphyrin was characterized by IR and UV-Vis spectroscopies and elemental analysis. All experiments were run in the phosphate buffer at pH 7.0. The buffer solution consisted of 5 mM Na_2HPO_4 and NaH_2PO_4 dissolved in double distilled water. To prepare the ct-DNA stock solution, 1 mg of ct-DNA was dissolved in 5 ml phosphate buffer and was stirred overnight and stored at 4.0 °C. The concentration of ct-DNA was determined from its optical absorption using its molar absorption coefficients, $\varepsilon_{259nm} = 1.32 \times 10^4$ cm^{-1} M^{-1} (*i.e.* reported in molar base pair) [23]. The pH values were controlled using a Metrohm-691 pH-meter.

Optical Absorption

The absorption spectra were recorded on a Cary 500 scan UV-Vis/NIR spectrophotometer equipped with a temperature controller and thermocouple monitor using a temperature rise of 1 deg min^{-1}. The $[Ni(II)(TF_4TMAPP)]^{4+}$ solutions were prepared in the concentration range of 1.72-13.8 μM for optical absorption measurements in the Soret band region. The UV-Vis titration experiments were made by the addition of the ct-DNA stock solution into a 1.4 ml cuvette containing $[Ni(II)(TF_4TMAPP)]^{4+}$ solution with appropriate concentration. The concentration range of ct-DNA was 10^{-6}-10^{-4} M. The titration experiments were performed at various temperatures with a precision of ±0.1 °C.

Fluorescence Spectroscopy

All fluorescence measurements were carried out with a Shimadzu model RF-5000 spectrofluorimeter by keeping the concentration of metalloporphyrin, $[Ni(II)(TF_4TMAPP)]^{4+}$ constant while varying the ct-DNA concentration from 0 to 2.90×10^{-5}, 4.29×10^{-5}, 5.38×10^{-5}, 628×10^{-5}, 7.02×10^{-5}, 8.85×10^{-5} and 9.64×10^{-5} M.

Resonance Light Scattering

The light scattering measurements were done on a Shimadzu model RF-5000 spectrofluorimeter. The scattered light intensity was monitored using the right angle in the synchronous scanning regime of the excitation and emission monochromators in the region of 300-600 nm. The experimental light-scattering spectra were corrected taking into account, the optical absorption of solution and instrument sensitivity dependence on the wavelength as described elsewhere [24,25]. All experimental data are the averaged values of at least five independent experiments.

Thermal Denaturation of ct-DNA

The thermal melting of ct-DNA was monitored on a Cary 500 scan UV-Vis/NIR spectrophotometer equipped with a temperature controller and thermocouple monitor using a temperature rise of 1 deg min^{-1}, at $\lambda = 259$ nm.

RESULTS AND DISCUSSION

Solution Properties of $[Ni(II)(TF_4TMAPP)]^{4+}$

In order to identify the solution properties of $[Ni(II)(TF_4TMAPP)]^{4+}$, we employed UV-Vis and RLS spectroscopic methods. The optical absorption spectrum of $[Ni(II)(TF_4TMAPP)]^{4+}$ shows three Q-bands and a B-Soret band feature, which is a characteristic of the base porphyrin (Fig. 1) [26]. Table 1 summarizes the molar absorptivity of these bands. The absorption in the Soret band obeys from Beer's law in the concentration range of 1.72-13.8 μM. These results suggest that $[Ni(II)(TF_4TMAPP)]^{4+}$ do not aggregate in the experimental concentration range.

The Effect of Ionic Strength

The effect of NaCl on the absorption spectrum of $[Ni(II)(TF_4TMAPP)]^{4+}$ (1×10^{-5} M) in water is shown in Fig. 2. The data concerning these spectral changes are presented in Table 2. As seen in Fig. 2, the bandwidth at half height, $W_{1/2}$ and the wavelength of maximum absorption, λ_{max} of the Q-band do not show considerable changes by increasing of NaCl concentration. However, as the concentration of NaCl increases, the absorbance at the Soret region of metalloporphyrin significantly exhibited

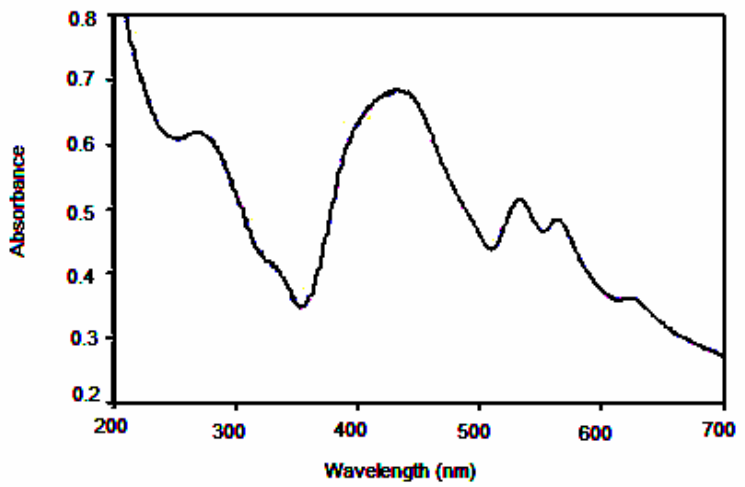

Fig. 1. Absorption spectrum of $[Ni(II)(TF_4TMAPP)]^{4+}$ solution (1×10^{-5} M) in 5 mM phosphate buffer, pH 7.0 and at 25.0 °C.

Table 1. UV-Vis Spectrum Characteristics of $[Ni(II)(TF_4TMAPP)]^{4+}$ in Aqueous Solution

Band	λ_{max} (nm)	ε ($M^{-1}cm^{-1}$)
Q-Band	622	3.63×10^4
Q-Band	563	3.58×10^4
Q-Band	533	3.79×10^4
B-Band	424	5.40×10^4

hypochromism with a little blue shift and decreasing of bandwidth. From these results, it can be concluded that $[Ni(II)(TF_4TMAPP)]^{4+}$ do not form defined aggregates due to increasing of ionic- strength [26].

Resonance Light Scattering

Resonance light scattering (RLS) is a useful technique to study electronically coupled chromophore arrays where enhanced light scattering of several orders of magnitudes can be observed at the absorption bands of the aggregates [27]. The scattered-light intensity (SLI) of a solution in the absence of optical absorption depends on the wavelength as $1/\lambda^4$ (Rayleigh law). The reason why this technique of resonance light scattering is considerably useful for aggregation experiments is that absorption and scatteringdepend on the size of the aggregate in very

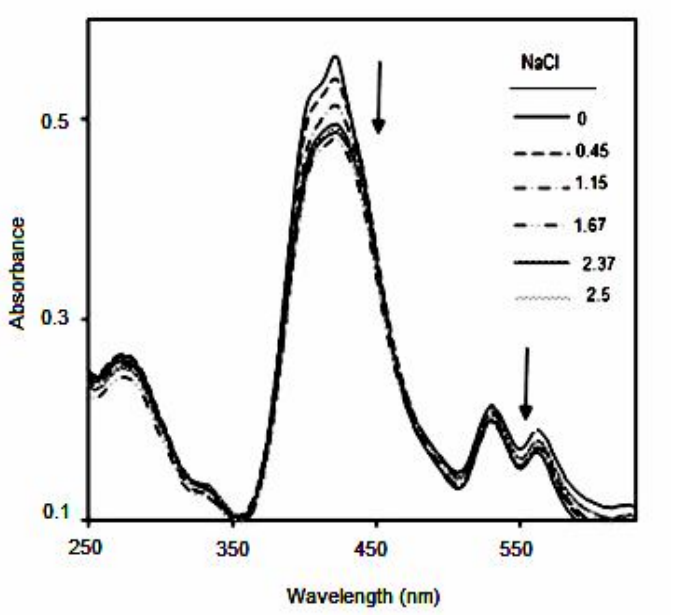

Fig. 2. Absorption spectra of $[Ni(II)(TF_4TMAPP)]^{4+}$ solution (1×10^{-5} M) upon addition of NaCl in 5 mM phosphate buffer, pH 7 and 25.0 °C.

Table 2. UV-Vis Spectral Characteristics of $[Ni(II)(TF_4TMAPP)]^{4+}$ Solution (1×10^{-5} M) upon Increasing the NaCl Concentration

[NaCl] (M)	A_{max}	λ_{max} (nm)	$W_{1/2}$ (nm)
0	0.393	425	70.9
0.45	0.360	424.8	72.1
0.65	0.359	424.8	71.1
1.15	0.358	424.8	69.2
1.42	0.355	424.6	69.1
1.96	0.353	424.8	68.5
2.30	0.351	424.4	68.3

different ways. Imagine the case in which a fixed concentration of material is under study. The absorption due to each sphere is proportional to the volume of the sphere, but the number of spheres per unit volume is inversely related to the volume of the sphere. The amount of absorption is therefore independent of the size of the spheres. This is implied by the Beer-Lambert law, since the absorption for a fixed path length should depend on the concentration of the material in the sample and nothing else. On the other hand, the scattering due to each sphere is proportional to the square of the volume. Since the number density of spheres depends inversely on the volume, the amount of scattering is directly proportional to the volume of each sphere. Thus, the larger the aggregate produces the greater the scattering. The buffer and NaCl solutions in the absence of metalloporphyrin were not absorbed in the Spectral region studied. Figure 3 shows the RLS spectra of the mixture of $[Ni(II)(TF_4TMAPP)]^{4+}$ and ct-DNA in a 5

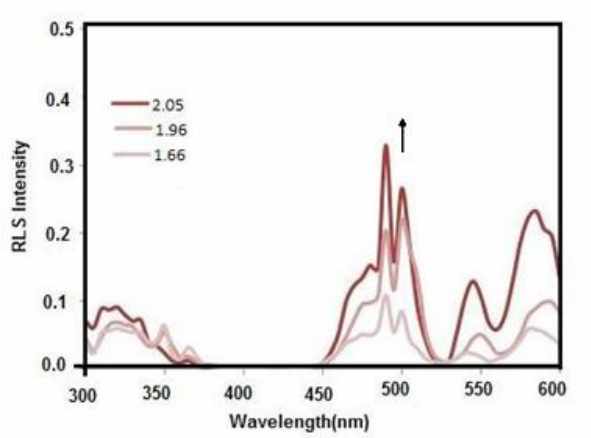

Fig. 3. The RLS spectra of $[Ni(II)(TF_4TMAPP)]^{4+}$ (1×10^{-5} M) in 5 mM phosphate buffer, pH 7.0 in 25.0 °C containing various concentration of ct-DNA.

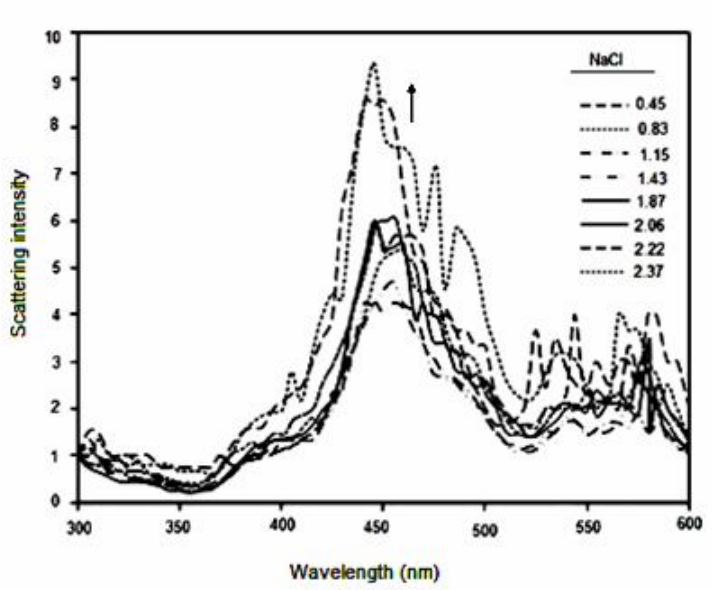

Fig. 4. The scattering intensity of $[Ni(II)(TF_4TMAPP)]^{4+}$-ct-DNA in 5 mM phosphate buffer pH 7.0 in the presence of various concentrations of NaCl.

mM phosphate buffer of pH 7.0 .

The ct-DNA solution alone had a weak RLS signal. However, when the ct-DNA was mixed with $[Ni(II)(TF_4TMAPP)]^{4+}$, the RLS signal was enhanced remarkably, indicating the probable interaction between $[Ni(II)(TF_4TMAPP)]^{4+}$ and ct-DNA According to the RLS theory, the intensity of RLS is related to the extent of the electronic coupling among chromophores and the particle dimension of the formed aggregate. Figure 4 shows that the ionic strength also affects the RLS intensity. It shows the RLS spectra of $[Ni(II)(TF_4TMAPP)]^{4+}$-ct-DNA solution, in 5 mM phosphate buffer of pH 7.0 in the presence of different NaCl concentrations. At the low ionic strength and in the absence of NaCl, only negligible RLS was observed in the Soret band spectral region. However, the RLS intensity of $[Ni(II)(TF_4TMAPP)]^{4+}$-ct-DNA at high ionic strength decreases with increasing NaCl concentration.

Fluorescence Spectroscopic Studies

To further investigate the interaction mode between the

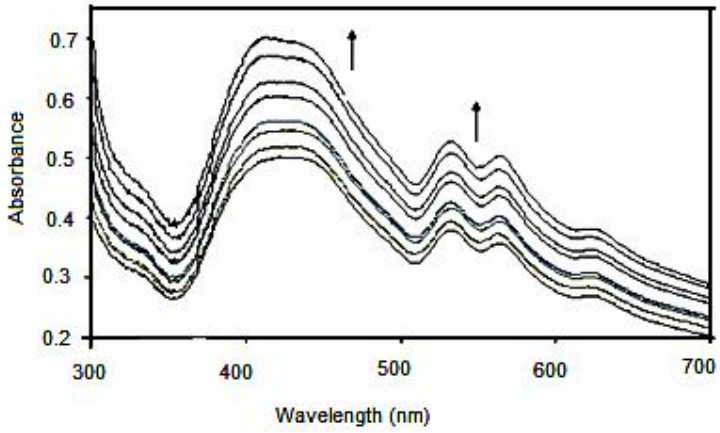

Fig. 5. The titration absorption spectra of $[Ni(II)(TF_4TMAPP)]^{4+}$, (1×10^{-5} M) in 5 mM phosphate buffer, pH 7.0 in 25.0 °C containing various concentration of ct-DNA. Concentration of ct-DNA: 0, 2.90×10^{-5}, 4.29×10^{-5}, 5.38×10^{-5}, 628×10^{-5}, 7.02×10^{-5}, 8.85×10^{-5} and 9.64×10^{-5} M, respectively.

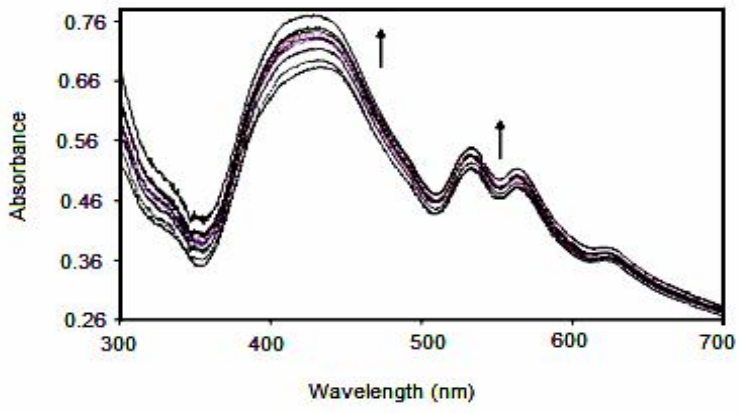

Fig. 6. The titration absorption spectra of $[Ni(II)(TF_4TMAPP)]^{4+}$, (1×10^{-5} M) in 5 mM phosphate buffer, pH 7.0 and 30.0 °C containing various concentration of ct-DNA. Concentration of ct-DNA: 0, 4.29×10^{-5} M, 5.85×10^{-5} M, 628×10^{-5} M, 7.02×10^{-5} M, 7.65×10^{-5} M, 8.42×10^{-5} M, 8.85×10^{-5} M and 9.64×10^{-5} M respectively.

metalloporphyrin and ct-DNA, fluorescence titration experiments were performed. The $[Ni(II)(TF_4TMAPP)]^{4+}$ exhibited fluorescence character in phosphate buffer with maximum wavelengths of about 278 nm. Figure 8 shows the emission spectra of the $[Ni(II)(TF_4TMAPP)]^{4+}$ in the absence and presence of varying amounts of ct-DNA. The emission intensity of $[Ni(II)(TF_4TMAPP)]^{4+}$ decreased regularly with growing amounts of ct-DNA and there was a blue shift of emission wavelength (278-272 nm). The results indicated that ct-DNA could quench the intrinsic fluorescence of $[Ni(II)(TF_4TMAPP)]^{4+}$ and the binding of $[Ni(II)(TF_4TMAPP)]^{4+}$ to ct-DNA indeed exists. The binding constant K and the number of binding sites n of $[Ni(II)(TF_4TMAPP)]^{4+}$ with ct-DNA were calculated by the following equation using the data from fluorescence titration [28]:

$$\text{Log}F_0 - F/F = \log K + n\log[\text{DNA}] \quad (1)$$

Here F_0 and F are the fluorescence intensities of the

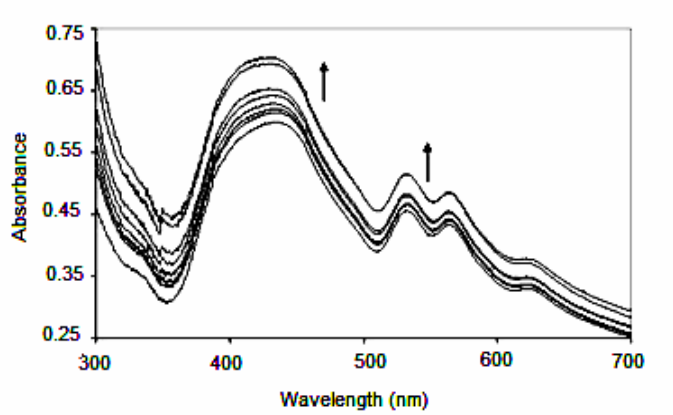

Fig. 7. The titration absorption spectra of $[Ni(II)(TF_4TMAPP)]^{4+}$, (1×10^{-5} M) in 5 mM phosphate buffer, pH 7.0 and 35.0 °C containing various concentration of ct-DNA. Concentration of ct-DNA: 0, 4.29×10^{-5} M, 5.38×10^{-5} M, 628×10^{-5} M, 7.92×10^{-5} M, 8.85×10^{-5} M and 9.64×10^{-5} M respectively.

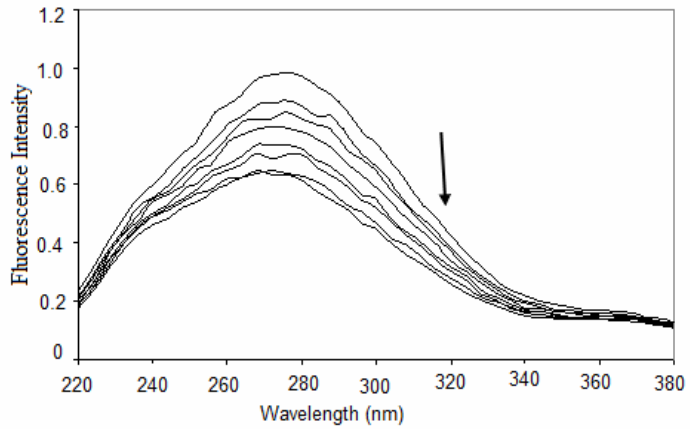

Fig. 8. Fluorescence emission spectra of $[Ni(II)(TF_4TMAPP)]^{4+}$ in the absence and presence of ct-DNA ($0\text{-}10^{-4}$ M) in 5 mM phosphate buffer pH 7.0. The arrow indicates the fluorescence intensity change with increasing of ct-DNA concentration.

$[Ni(II)(TF_4TMAPP)]^{4+}$ in the absence and the presence of different concentrations of ct-DNA, respectively. [DNA] represents the concentration of ct-DNA, *K* is the binding constant and *n* is the number of the binding sites, which can be determined by the ordinate and the slope of the double logarithm regression curve (Fig. 9) of $\log(F_0\text{-}F)/F$ *vs.* log[DNA] based on the Eq. (1), respectively. The values of *K* and *n* were found to be 2.4×10^3 M^{-1} and 0.6198 at 298 K, respectively.

THE BINDING OF [NI (II) $(TF_4TMAPP)]^{4+}$ TO CT-DNA

Analysis of the Optical Absorption Spectrum

The optical absorption spectrum of $[Ni(II)(TF_4TMAPP)]^{4+}$ shows three Q bands and a Soret band feature. Beer's Law experiments were carried out for metalloporphyrin in homogeneous aqueous solution at pH = 7. 0 and the molar absorptivity of these bands was also calculated. The fixed amount of cationic metalloporphyrin, $[Ni(II)(TF_4TMAPP)]^{4+}$ (1×10^{-5} M) in 5 mM phosphate buffer of pH 7.0 was titrated with varying concentrations of ct-DNA at various temperatures. The spectral feature of the studied metalloporphyrin at various ct-DNA concentrations and temperatures are shown in Figs. 5-7. As shown in these figures, the intensity of the Soret band (424 nm) and Q bands regions (622, 563, 533 nm) are increased regularly with growing amounts of ct-DNA and there is a little blue shift of the absorption wavelength at Soret band. These changes reveale that the interaction of $[Ni(II)(TF_4TMAPP)]^{4+}$ with ct-DNA does occur. Moreover, there are no isosbestic points in titration spectra of

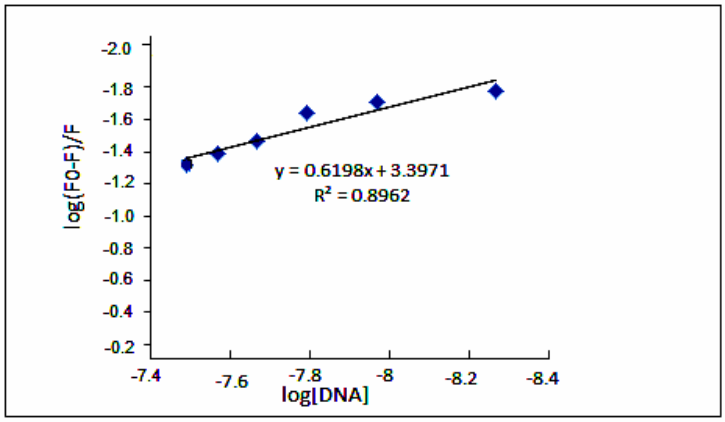

Fig. 9. The plot of $\log(F_0\text{-}F)/F$ *vs.* log[ct-DNA].

Table 3. Thermodynamic Parameters and Affinity Constants for Binding of $[Ni(II)(TF_4TMAPP)]^{4+}$ to ct-DNA at 5 mM Phosphate Bufer, pH 7.0 and Various Temperatures

T (K)	$\log K_1$ (M^{-1})	ΔG_1^o (kJ mol^{-1})	ΔH_1^o (kJ mol^{-1})	ΔS_1^o (J mol^{-1} K^{-1})
298.0	5.20 ± 0.17	-29.67 ± 0.97	61.31 ± 16.23	305.31 ± 57.71
303.0	5.33 ± 0.26	-30.92 ± 1.51	61.31 ± 16.23	04.41 ± 58.54
308.0	5.58 ± 0.17	-32.91 ± 1.00	61.31 ± 16.23	305.91 ± 55.94
313.0	5.66 ± 0.31	-33.92 ± 1.86	61.31 ± 16.23	304.26 ± 57.78
318.0	5.88 ± 0.37	-35.80 ± 2.25	61.31 ± 16.23	305.39 ± 58.12

$[Ni(II)(TF_4TMAPP)]^{4+}$. Generally, hypochromic and red shift are observed in the absorption spectra of small molecules if they intercalate the base pairs [29], however the hyperchromic effect was found in the UV-Vis spectra, revealing that $[Ni(II)(TF_4TMAPP)]^{4+}$ binding to ct-DNA would be probably outside binding mode [30].

The binding constant at any specified temperature was determined by the concentration dependence of UV-Vis absorption data using SQUAD program. This program has been developed for evaluation of the best set of binding constants of the proposed equilibrium model by employing a non-linear least-squares approach. The input data consists of (a) the absorbance values, (b) the total ct-DNA and metalloporphyrin concentrations. The absorption data were analyzed by assuming 1:1 or 2:1 and/or simultaneously 1:1 and 2:1 molar ratios of metalloporphyrin to ct-DNA. Fitting of the experimental data (15 point) to the proposed stoichiometric models was evaluated by the sum of squares of the calculated points by the model. The results show that the most suitable case corresponds to 1:1 and 2:1 combining models at range of the studied temperatures [31]. The calculated binding constants are given in Table 3 and 4. These results represent the increasing of binding constants with increasing of temperature. The *K* value indicates a high binding affinity of $[Ni(II)(TF_4TMAPP)]^{4+}$ for DNA and the existence of outside or groove binding between DNA and porphyrin complex.

Thermodynamic Studies

A prerequisite for deeper insight into the molecular basis of metalloporphyrin-DNA interactions is thorough characterization of the energetics governing the complex formation. The energetics of $[Ni(II)(TF_4TMAPP)]^{4+}$-ct-DNA equilibrium can be conveniently characterized by three thermodynamic parameters, standard Gibbs free energy, $\Delta G°$, standard enthalpy, $\Delta H°$ and standard entropy

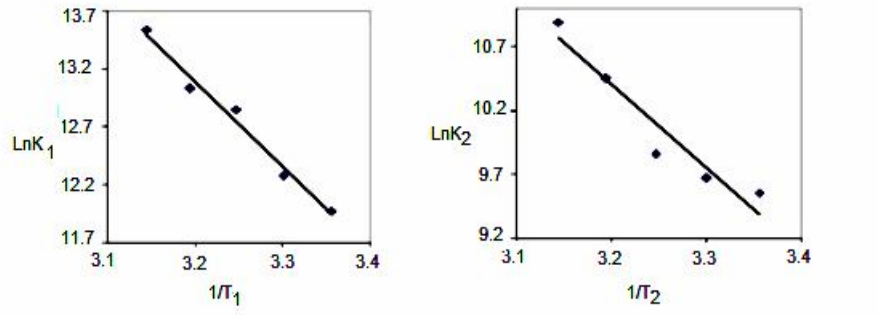

Fig. 10. The van't Hoff plot $[Ni(II)(TF_4TMAPP)]^{4+}$ binding to ct-DNA.

Table 4. Thermodynamic Parameters and Affinity Constants for Binding of $[Ni(II)(TF_4TMAPP)]^{4+}$ to ct-DNA at 5 mM Phosphate Buffer, pH 7.0 and Various Temperatures

T (K)	LogK_2 (M^{-1})	ΔG_2^o (kJ mol^{-1})	ΔH_2^o (kJ mol^{-1})	ΔS_2^o (J mol^{-1} K^{-1})
298.0	4.15 ± 0.09	-23.68 ± 0.51	54.15 ± 8.14	181.80 ± 29.05
303.0	4.20 ± 0.11	-24.37 ± 0.64	54.15 ± 8.14	178.80 ± 28.98
308.0	4.28 ± 0.12	-25.24 ± 0.71	54.15 ± 8.14	175.90 ± 28.74
313.0	4.45 ± 0.00	-27.21 ± 0.00	54.15 ± 8.14	173.10 ± 26.02
318.0	4.73 ± 0.2.6	-28.80 ± 1.58	54.15 ± 8.14	170.38 ± 30.59

changes, $\Delta S°$. $\Delta G°$ can be calculated from the equilibrium constant, K, of the reaction using the familiar relationship, $\Delta G° = -RT \ln K$, in which R and T refer to the gas constant, and the absolute temperature, respectively. Furthermore, K is the apparent equilibrium constant and consequently $\Delta G°$ is the apparent Gibbs free energy change. If heat capacity changes for the reaction are essentially zero, the van't Hoff equation (Eq. (2)) gives a linear plot of $\ln K$ *vs.* $1/T$ (Fig. 8) [32].

$$d\ln K/d(1/T) = -\Delta H°/R \quad (2)$$

The apparent standard enthalpy change $\Delta H°$ can be calculated from the slope of the straight line, $-\Delta H°/R$ and the apparent standard entropy change from its intercept, $\Delta S°/R$. The van't Hoff plots for interaction of $[Ni(II)(TF_4TMAPP)]^{4+}$ with ct-DNA is shown in Fig. 10. The calculated thermodynamic parameters for binding of $[Ni(II)(TF_4TMAPP)]^{4+}$ to ct-DNA are listed in Tables 3 and 4. It has been revealed that the standard Gibbs free energy changes for $[Ni(II)(TF_4TMAPP)]^{4+}$-ct-DNA interaction is negative, representing the relative affinity of the $[Ni(II)(TF_4TMAPP)]^{4+}$ complex to ct-DNA. It has been also indicated that the binding process is endothermic disfavored ($\Delta H° > 0$) and entropy favored ($\Delta S° > 0$). As proposed by Ross [33], when $\Delta H° < 0$ or $\Delta H° \approx 0$, $\Delta S° > 0$, the mainly acting force is electrostatic, when $\Delta H° < 0$, $\Delta S° < 0$, the mainly acting force is van der Waals or hydrogen bonding and when $\Delta H° > 0$, $\Delta S° > 0$, the main force is hydrophobic. Therefore, in the cases of the present system, we presumed that hydrophobic interaction might be the main acting force in the binding of the $[Ni(II)(TF_4TMAPP)]^{4+}$ and ct-DNA. Thermodynamic data clerely shows that the interaction processes are endothermic disfavored, but entropy favored ($\Delta H° > 0$, $\Delta S° > 0$). These results illuminated that the interactions between ct-DNA and $[Ni(II)(TF_4TMAPP)]^{4+}$did not follow the traditional intercalating mode, while the conformation changes of ct-DNA structure may be realized *via* entropy driven non-classical intercalation interaction.

Thermal Denaturation of ct-DNA

Another strong evidence for the binding mode between the complexes and ct-DNA was obtained from ct-DNA melting (T_m) studies by investigating the UV-Vis spectra of $[Ni(II)(TF_4TMAPP)]^{4+}$-ct-DNA at different temperatures. The melting curves of both free ct-DNA and $[Ni(II)(TF_4TMAPP)]^{4+}$-ct-DNA in phosphate buffer was obtained by measuring the hyperchromicity of ct-DNA absorbance at 259 nm as a function of temperature. The temperature was scanned from 24.0-86.0 ºC at a speed of 0.4.0 °C min^{-1}. The melting temperature (T_m) was taken as the midpoint of the hyperchromic transition. The melting temperature (T_m) of ct-DNA is sensitive to its double helix stability, and binding of the compounds to ct-DNA alters

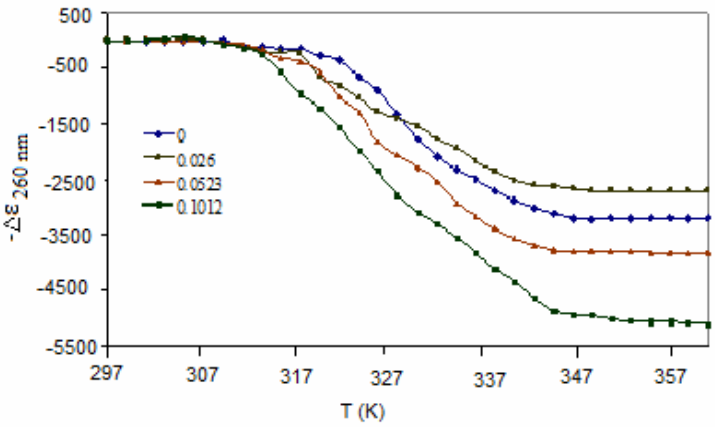

Fig. 11. Melting profiles ($\lambda_{detection}$ = 260 nm) for the free ct-DNA in the absence of and presence of $[Ni(II)(TF_4TMAPP)]^{4+}$ and for the different molar ratios of ct-DNA and $[Ni(II)(TF_4TMAPP)]^{4+}$ in the temperature range of 24.0- 86.0 °C.

the T_m values depending on the strength of the interactions. The difference between the melting temperatures of DNA in a buffer solution and DNA with a ligand is large if binding of the ligand to DNA occurs through intercalation. On the other hand, if the binding mode of the ligand to DNA is non-intercalative, the difference in the melting temperatures is smaller [34,35]. In our experiments, the obtained data show that the interaction of the studied metalloporphyrin ($[Ni(II)(TF_4TMAPP)]^{4+}$) with ct-DNA leads to relatively moderate stabilization of the ct-DNA structure. Moreover, the increase in metalloporphyrin-to-ct-DNA concentration ratio weakly affects T_m of the melting curve. As shown in Fig. 9, T_m is decreased to 328.5 K, 326.7 K, 326.3 K and 323.1 K with the ratios of $[Ni(II)(TF_4TMAPP)]^{4+}$ to ct-DNA at 0, 0.026, 0.052 and 0.1012, respectively. These results show that T_m of the system with $[Ni(II)(TF_4TMAPP)]^{4+}$ added is not increased as it is observed for daunomycin [36] cryptolepine [37] and chlorobenzylidine [38], confirming that their interaction with ct-DNA should be intercalative made. The results also support that the binding modes of $[Ni(II)(TF_4TMAPP)]^{4+}$ with ct-DNA is non-traditional intercalated. The small decrease of T_m might be due to the interaction of $[Ni(II)(TF_4TMAPP)]^{4+}$ with ct-DNA *via* outside binding interaction [39] (Fig. 11).

CONCLUSIONS

In this work, we present a comprehensive study of the interaction between ct-DNA and a cationic metalloporphyrin $[Ni(II)(TF_4TMAPP)]^{4+}$. The interactions of $[Ni(II)(TF_4TMAPP)]^{4+}$ with ct-DNA have been studied at physiological pH 7.0 using UV-Vis and fluorescence spectroscopic techniques, ct-DNA melting techniques and RLS measurements. By the analysis of UV-Vis spectra, it was found that the interacting forces between $[Ni(II)(TF_4TMAPP)]^{4+}$ and ct-DNA include outside interaction. Moreover, the binding constants and thermodynamic parameters were calculated. From the fluorescence spectra, the binding constant and the number of binding sites were obtained. The thermal denaturation study suggested that the interaction of the studied metalloporphyrin ($[Ni(II)(TF_4TMAPP)]^{4+}$) with ct-DNA leads to relatively moderate stabilization of the ct-DNA structure. Moreover, the increase in metalloporphyrin-to-ct-DNA concentration ratio weakly affects T_m of the melting curve. All observations were consistent with an outside electrostatic binding mode for $[Ni(II)(TF_4TMAPP)]^{4+}$. This work could help us to go further in understanding the binding mechanism of $[Ni(II)(TF_4TMAPP)]^{4+}$ with ct-DNA and designing the structure of new and efficient drug molecules targeted to ct-DNA.

ACKNOWLEDGMENTS

We are grateful to the Research Council of Yazd University and Payame Noor University for their financial supports. The authors would like to express their great appreciation to Professor A.K. Bordbar for good cooperation.

REFERENCES

[1] P. Hambright, E.B. Fleicher, Inorg. Chem. 9 (1970) 1757.

[2] R.J. Fiel, J.C. Howard, E.H. Mark , N. Datta-Gupta, Nucleic Acids Res. 6 (1979) 3093.

[3] I. Haq, J.O .Trent, B Z. Chowdhry, T.C. Jenkins, J. Am. Chem. Soc. 121 (1999) 1768.

[4] M. Sirish, H.J. Schneider, Chem. Commun. (1999) 907.

[5] G. Pratviel, J. Bernadou B. Meunier, Met. Ions Biol. Syst. 33 (1996) 399.

[6] E. Di Mauro, R. Saladino, P. Tagliatesta, V. De Sanctis, R. Negri, J. Mol. Biol. 282 (1998) 43.

[7] R.J. Fiel, J. Biomol. Struct. Dyn. 6 (1989) 1259.

[8] L.G. Marzilli, New J. Chem. 14 (1990) 409.

[9] R.F. Pasternack , E.J. Gibbs, Met. Ions Biol. Syst. 33 (1996) 367.

[10] N.E. Makundan, G. Petho, D.W. Dixon, L.G. Marzilli, Inorg. Chem. 34 (1995) 3677.

[11] P. Zhao, J.W. Huang, L.N. Ji, Spectrosc. Lett. 44 (2011) 211.

[12] M. Nejat, A.K. Bordbar, P. Lincoln, V. Mirkhani, Spectrochim. Acta, Part A. 90 (2012) 50.

[13] N. Robic, C. Bied-Charreton, M. Perree-Fauvet, C. Verchere-Beaur, L. Salmon, A. Gaudemer, R.F. Pasternack, Tetrahedron Lett. 31 (1990) 4739.

[14] A. Salehi, H.Y. Mei, T. Briuce, Tetrahedron Lett. 32 (1991) 3453.

[15] M. Perree-Fauvet, N. Gresh, Tetrahedron Lett. 36 (1995) 4227.

[16] T. Goslinski, J. Piskorz, J. Photochem. Photobiol. C: Photochem. Rev. 12 (2011) 304.

[17] M. Tabat, A.K. Sarker, E. Nyarko, J. Inorg. Biochem. 94 (2003) 50.

[18] C. Uslan, B.S. Sesalan, Dyes Pigm. 94 (2012) 127.

[19] R.F. Pasternack, P. Garrity, B. Ehrlich, C.B. Davis, E.J. Gibbs, G. Osloff, A. Giartosio, C. Turano, Nucleic Acids Res.14 (1986) 5919.

[20] A. Villanueva, G. Jori, Cancer Lett. 73 (1993) 59.

[21]] L.T. Richards, G.M. Miskelly, Inorg. Chem. 33 (1994) 3159.

[22] K.M. Kadish, C. Araullo-McAdams. B.C. Han, M.M. Franzen, J. Am. Chem. Soc. 112 (1990) 8364.

[23] R.F. Pasternack, C.B. Bustamante, P.J. Collings, A. Giannetto, E.J. Gibbs, J. Am. Chem. Soc. 115 (1993) 5393.

[24] I.E .Borissevitch, T.T .Tominaga, H. Imasato, M. Tabak, Anal. Chem. Acta 343 (1997) 281.

[25] A.K. Bordbar, A. Eslami, S. Tangestaninejad, J. Porphyr. Phthalocyanines. 6 (2002) 225.

[26] R. Tehhuneu, H.S. Mavver, J. Biol. Chem. 244 (1969) 6388.

[27] K. Kano, H. Minamizono, T. Kitae, S. Negi, J. Phys. Chem A 101 (1997) 6118.

[28] R. Bera, B.K. Sahoo, K.S. Ghosh, S. Dasgupta, Int. J. Biol. Macromol. 42 (2008) 14.

[29] E.C. Long, J. Barton, Acc. Chem. Res. 23 (1990) 271.

[30] H. Dezhampanah, A.K. Bordbar, Sh. Tangestaninejad, J. Porphyrins Phthalocyanines. 13 (2009) 964.

[31] N. Tajdini, A. Moghimi, Orient J. Chem. 26 (2010) 843.

[32] N. Mudasir, N. Yoshioka, H. Inoue, J. Inorg. Biochem. 77 (1999) 239.

[33] P.D. Ross, S. Subramanian, Biochem. 20 (1981) 3096.

[34] D. Zeynep, P. Ralph, A.R.S. Jan, N. Sukunath, R. Clemens, J. Am. Chem. Soc. 126 (2004) 4762.

[35] Y.Q. Li, J. White, S. David, S. Gary, S. Michael, Biotechnol. Prog. 17 (2001) 348.

[36] J.B. Chaires, N. Dattagupta, D.M. Crothers, Biochem. 21 (1982) 3933.

[37] K. Bonjean, M.C. de Pauw-Gillet, M.P. Defresne, Biochem. 37 (1998) 5136.

[38] W. Zhong, J. Yu, Y. Liang, K. Fan, L. Lai, Spectrochim. Acta A 60 (2004) 2985.

[39] S.A.S. Sulyman, A.A. Ghazaryan, Y.B. Dalyan, Am. J. Phys. 2 (2009) 139.